SUPPORTING MATERIAL

Protrusion fluctuations direct cell motion

*David Caballero [1,2], Raphaël Voituriez [3,4], Daniel Riveline [1,2 *]*

[1] Laboratory of Cell Physics, ISIS/IGBMC, Université de Strasbourg and CNRS (UMR 7006), 8 allée Gaspard Monge, 67083 Strasbourg, France

[2] Development and Stem Cells Program, IGBMC, CNRS (UMR 7104), INSERM (U964), Université de Strasbourg, 1 rue Laurent Fries, BP10142, 67400 Illkirch, France

[3] Laboratoire de Physique Théorique de la Matière Condensée, CNRS UMR 7600, Université Pierre et Marie Curie, 4 Place Jussieu, 75005 Paris, France

[4] Laboratoire Jean Perrin, CNRS FRE 3231, Université Pierre et Marie Curie, 4 Place Jussieu, 75005 Paris, France

[*]Corresponding author: Daniel Riveline; e-mail: riveline@unistra.fr, Laboratory of Cell Physics, ISIS/IGBMC, Université de Strasbourg and CNRS (UMR 7006), 8 allée Gaspard Monge, 67083 Strasbourg, France. TEL: +33 (0) 3 68 85 51 64; FAX: +33 (0) 3 68 85 52 32.

1. Supplementary Material and Methods

Fibronectin concentration: The fibronectin concentration (10 μg ml^{-1}) was selected in the following manner. The velocities of cells were measured for various concentrations on homogeneously coated microcontact-printed surfaces (see Fig. S3). As reported by Palecek *et al*, a dumbbell shape was recorded for the velocity-concentration plot with saltatory NIH3T3 cells in the lower region and crawling NIH3T3 cells in the higher density region (see ref. (23) in the main text). To obtain long displacements for long-term motion, we selected the higher speeds while keeping the cells in the crawling regime.

Data analysis: We measured biophysical parameters in the following manner. Cells trajectories were tracked manually by clicking on the centroid of each cell (Manual Tracking Plug-in, ImageJ) at 5 minute intervals for 48 hours. Points were connected to generate the migration path. Specifically, we used this method to extract L_p, T_p, v and T_{pa} (a definition of these parameters is included in the Materials and Methods section in the main manuscript). Nt^{-1} was recorded as the number of turns that cells performed during their full motion. Note that N is given by $1/(T_p+T_{pa})$; v is the ratio of $\langle L_p^i/T_p^i \rangle$, where i=1..n cells, and v is different from $\langle L_p \rangle / \langle T_p \rangle$ because the distributions are not Gaussian. To classify the motions as +/–/null (no net motion), the cell positions at the start and the end of the movies were compared. 'No net motion' corresponded to cells returning to the original pattern location, although the cells had been fluctuating + and - during the acquisition. The data are provided as the mean ± SEM. Statistical analysis was performed using Student's *t*-test, and significance was accepted at $P<0.05$.

Cell fixation and staining: Cells were fixed with 3% paraformaldehyde (Sigma-Aldrich, France) at 37°C for 17 min or with methanol at -20°C for 10 min for centrosome fixation. Then, 0.5%

Triton (Sigma-Aldrich, France) was added for 3 min to permeabilize the cells, and the samples were washed twice for 5 min with 1X PBS. For staining, we used Alexa Fluor 488-phalloidin (Molecular Probes) for actin, rabbit anti-pericentrin (Covance, UK) for the centrosome, and DAPI (4.6-diamidino-2-phenylidole, Sigma-Aldrich, France) for the nucleus. Focal contacts were stained with mouse anti-paxillin (Sigma-Aldrich, France), and microtubules were stained with mouse monoclonal anti-alpha tubulin (Sigma-Aldrich, France). The following secondary antibodies were used: goat anti-mouse conjugated with Cy3, Alexa 488 goat anti-rabbit (Molecular Probes, France) and Alexa Fluor 647 goat anti-mouse (Fisher Scientific SAS, France). The incubations with antibodies were performed for 45 min at room temperature in PBS. To stain the focal contacts on the pattern, incubation was conducted in PBS with 3% BSA. The stained samples were observed with an inverted fluorescence microscope (Eclipse Ti, Nikon, Japan) combined with a Photometrics CoolSNAP HQ^2 camera. We used a pre-centered fiber illuminator (C-HGFIE, Nikon, Japan) and a X60 oil objective (Nikon, Japan) with a numerical aperture of 1.3.

2. Supplemental Figures and Legends.

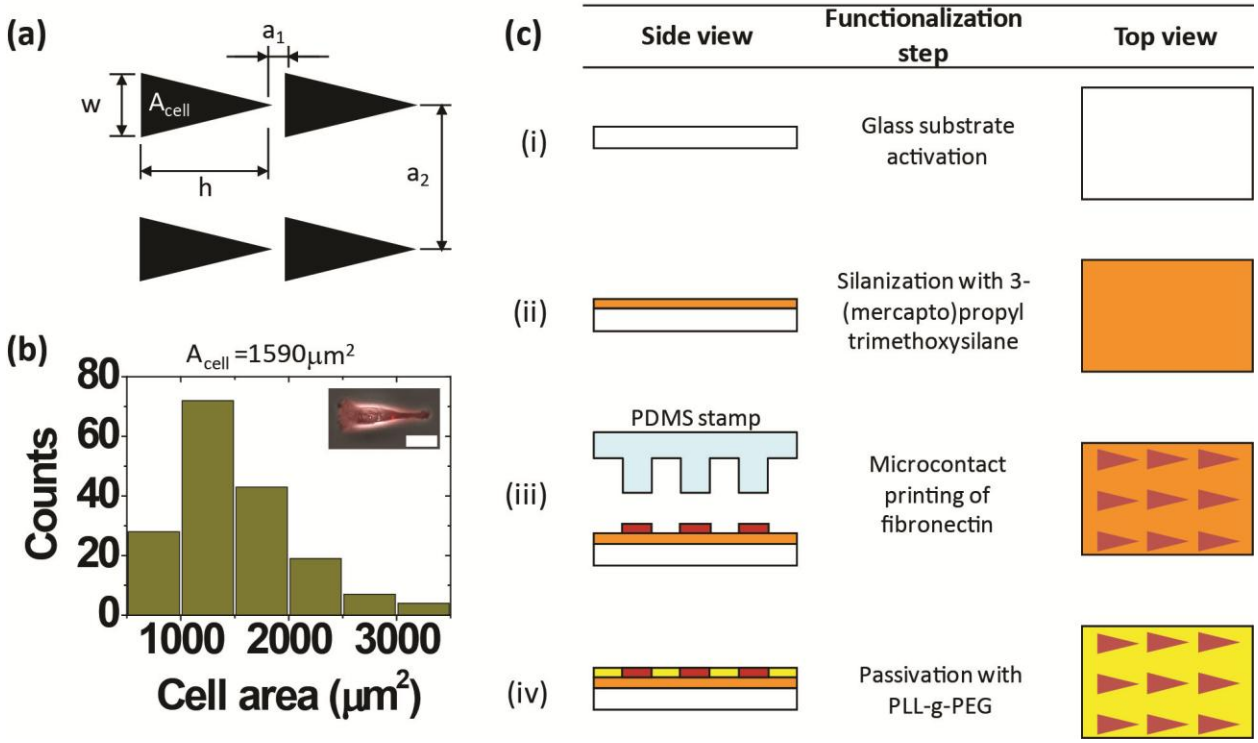

Fig. S1. Ratchet design and protocol for its fabrication. (a) Micropattern design showing the different values used. *w=30 μm; h=106 μm; a_1=20.5 μm; a_2=200 μm* and *A=1590 μm²*. **(b)** Optimization of the micropattern area. Cells were deposited on a microcontact printed glass coverslip with a 10 μg ml^{-1} fibronectin concentration and were allowed to spread. The area of individuals cells (n=176 cells) was measured, and the averaged A_{cell}*=1590±54μm²* was selected for the motif design. Inset, a cell completely spread on a single asymmetric fibronectin motif. Scale bar = 35 μm. **(c)** Functionalization protocol (see Methods). *(i)* Glass coverslips, #1, were thoroughly cleaned and chemically activated with *'Piranha'* solution. *(ii)* Glass coverslips were silanized by vapor phase deposition with 3-(mercapto)propyl trimethoxysilane and placed in an oven at 65°C for 4 hours. *(iii)* The microcontact printing technique was used to deposit fibronectin patterns on the substrates. *(iv)* Non-functionalized regions were passivated with poly(L-lysine)-g-poly(ethylene glycol) (PLL-g-PEG). Samples were stored in PBS (pH 7.4) at 4°C for at least 30 minutes prior to use.

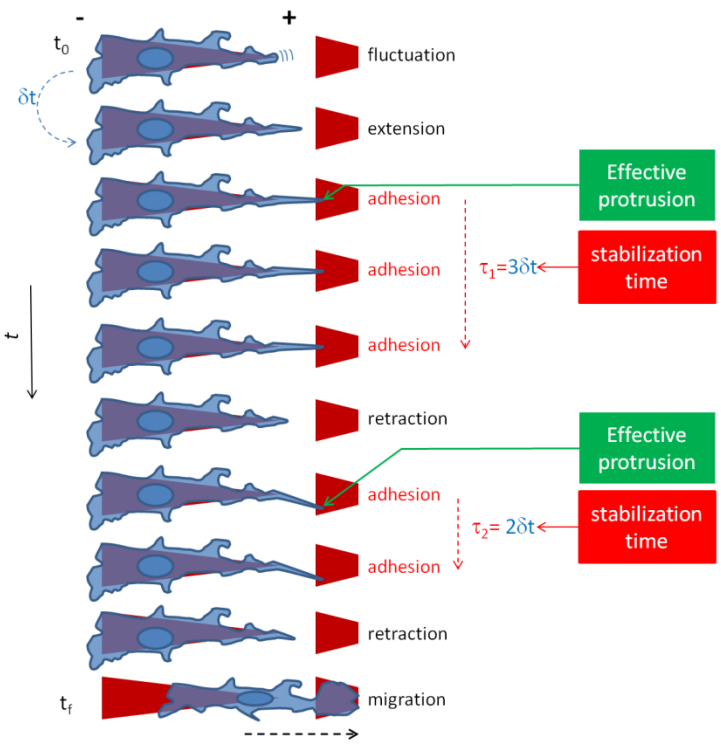

Fig. S2. Scheme showing the definitions of ν and τ. A cell protrusion fluctuates, grows and adheres (effective protrusion) on the neighboring motif during τ_1 and τ_2 before retracting and migrating towards the + direction. δt represents the time between acquisitions, and t_0 and t_f represent the start and end of the experiment, respectively.

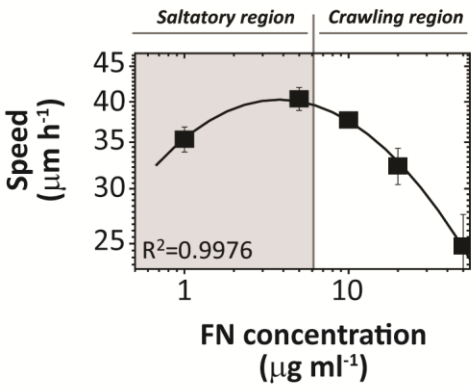

Concentration ($\mu g\ ml^{-1}$)	Speed ($\mu m\ h^{-1}$)	Number of cells
1	35.3 ± 1.5	269
5	40.4 ± 1.5	331
10	37.7 ± 0.9	369
20	32.4 ± 1.9	351
50	24.8 ± 2.7	373

Fig. S3. Representation of NIH3T3 cell migration speed as a function of fibronectin coating concentration. *(Left)* Variation of the mean speed of NIH3T3 cells on surfaces that were homogeneously coated with fibronectin (FN). The speed is measured by tracking the centroid of each individual cell: we compute the initial and final points where NIH3T3 cells are moving straight. We observed two different regimes: the first one ranged from $1 \leq [FN] < 6\ \mu g\ ml^{-1}$ (grey zone) with saltatory cells, and the second one ranged from $6 \leq [FN] \leq 50\ \mu g\ ml^{-1}$ (white zone) with crawling cells. The data correspond to N=6 independent experiments for at least 269 NIH3T3 cells per condition for a total of n=1693 cells. *(Right)* Table showing the speed obtained for each fibronectin concentration with the number of cells analyzed per condition. The values are shown as the mean ± SEM.

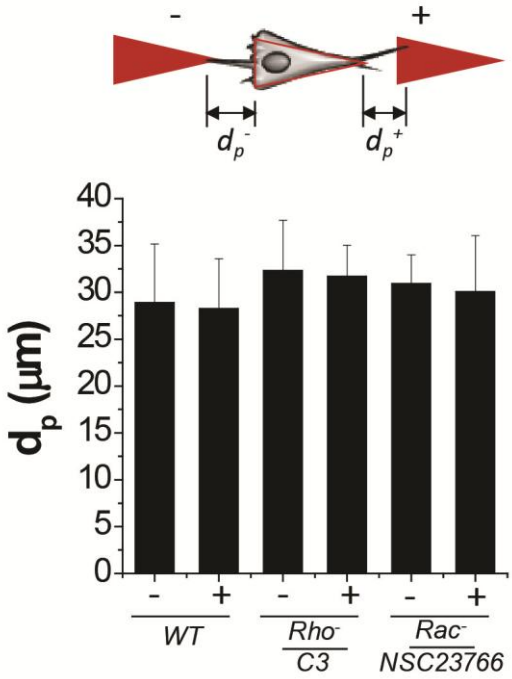

Fig. S4. Protrusion length extension. Average protruding distance d_p in the + and – directions. NIH3T3 cells extend filopodia protrusions of similar lengths in all directions for each condition. (Data set: *WT*=885; *C3-Rho*$^-$ = 1084 and *NSC23766-Rac*$^-$ = 1084 analyzed filopodia. N=3). The data are presented as the mean ± SD.

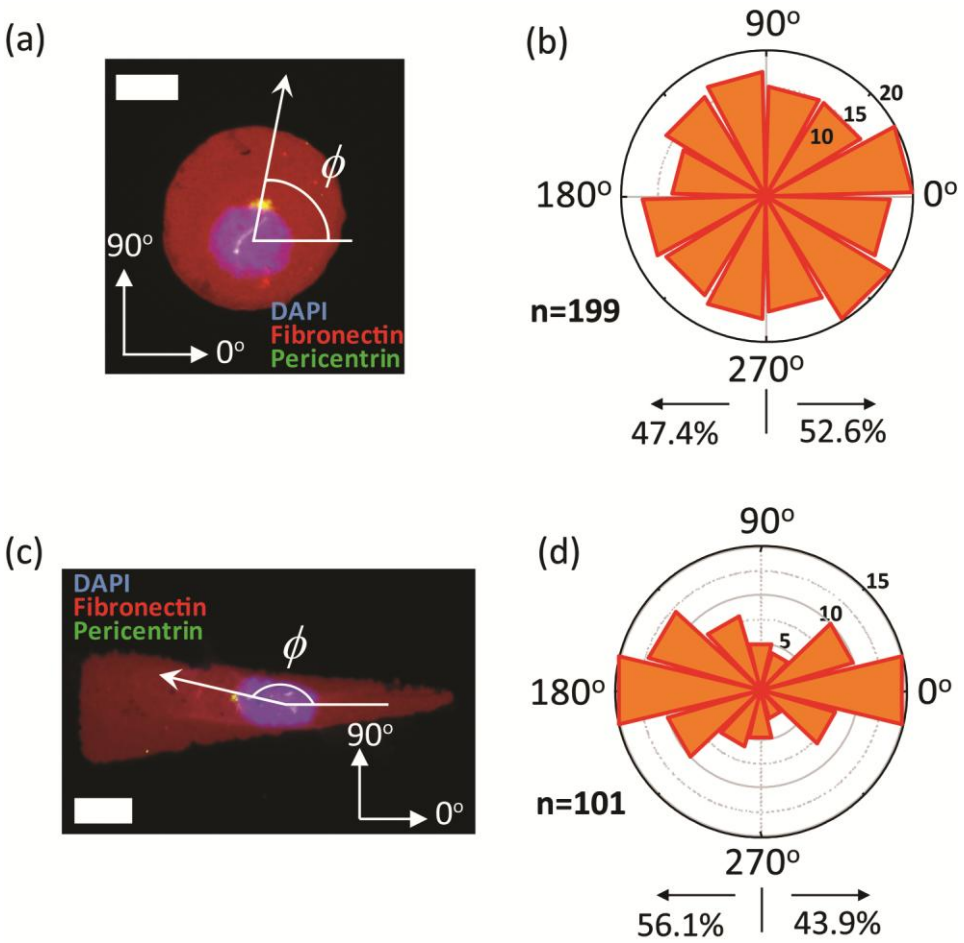

Fig. S5. Internal polarity caused by the asymmetric fibronectin motif. (a) NIH3T3 cells were allowed to spread prior to fixation. They were stained for the nucleus (blue) and centrosome (green). The centrosome positions were measured with respect to the nucleus (see Methods). Scale bar: 15 μm. **(b)** Circular histogram of the angular distributions for the centrosome with respect to the nucleus centroid (n=199 cells) for cells plated on fibronectin spots; the distribution is isotropic. **(c)** Fixation and staining for the nucleus (blue) and centrosome (green) of NIH3T3 cells on rhodamine-labelled asymmetric fibronectin (10 μg ml^{-1}) triangles. The centrosome positions were measured with respect to nucleus. Scale bar: 15 μm. **(d)** Circular histogram of the angular distributions of the centrosome with respect to the nucleus centroid (n=101 cells). The histogram shows a distribution of centrosomes along the longer cell axis and a bias towards the wide edge.

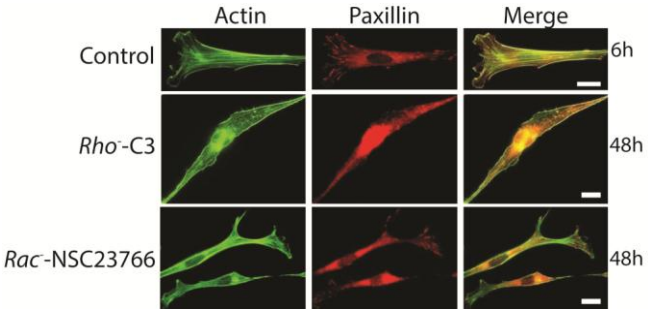

Fig. S6. Inhibiting the Rho and Rac pathways clearly affect the cytoskeleton. NIH3T3 cells were deposited on a microcontact printed glass coverslip with a 10 μg ml^{-1} fibronectin concentration. We compared the effects of inhibiting the Rho and Rac pathways on the cell cytoskeleton via treatments with the inhibitors C3 transferase (80 nM) and NSC23766 (100 μM), respectively. NIH3T3 cells were labeled for actin and paxillin. The right column shows the incubation time at fixation; note that similar phenotypes were observed for each condition throughout the experiments. Scale bar = 10 μm.

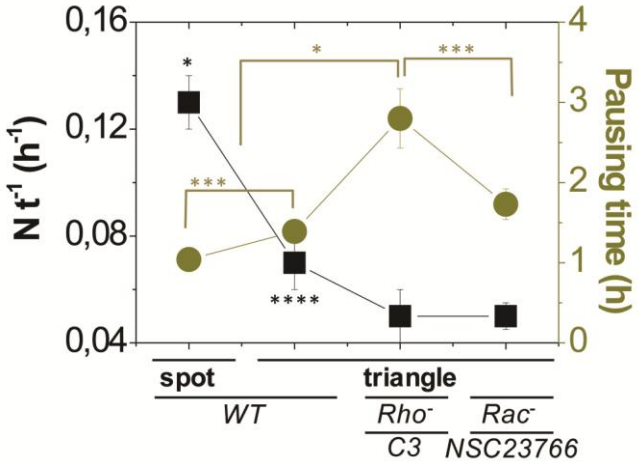

Fig. S7. Characterization of the long-term cell motion. *(Left)* Number of changes in the direction per unit time for all conditions. The cells switch direction more often for the *WT* spot condition. The data suggest a directional motion that lasts longer for the ratchet configuration with Rho^- and Rac^-. *(Right)* Pausing time (T_{pa}) prior to a change in direction for all conditions. For the Rho^- condition, the cells show the highest T_{pa} value. The data are presented as the mean±SEM. *$P<0.001$; ***$P<0.01$; ****$P<0.05$. (Student's *t*-test).

3. Supplementary Model Description

3.1 Probabilistic model for the direction index I_{dir} - first step motion

We present a simple model that predicts the probability p_+ that a protrusion is stabilized in the + direction rather than the − direction for a cell on a 1d lattice of triangular adhesive patterns. We show that direction index I_{dir} quantifies the asymmetry in this quantity: $I_{dir}= p_+ - p_-$. The width and height of a triangular region are h and w, respectively (we follow the notations in Fig. S1). The gap distance between the two nearest adhesive regions is a_1. Cells extend protrusions to the nearest adhesive regions on the + and - directions. The probability distribution that an extended protrusion has the length l has the form

$$\psi(l) = \lambda e^{-\lambda l} \tag{1}$$

where λ^{-1} is the average length of the protrusions. This exponential form for the probability distribution was shown experimentally by Xia *et al* (FASEB J. **22**:1649-1659 (2008)). Cells extend n_+ (multiple) protrusions towards the + direction and n_- protrusions towards the - direction at the same time (where $n_+ \neq n_-$ for the case of cells on triangular patterns because of cell polarization) with frequency $1/\tau_p$. The probability ψ_+ that a protrusion that extended towards the + direction touches the adhesive region at the nearest neighbor is derived by integrating $\psi(l)$ in the adhesive regions at the nearest neighbor and has the form

$$\psi_+ = g_+ e^{-\lambda a_1}, \tag{2}$$

where g_+ is the geometrical factor, which depends on h and w and which we do not aim at determining here. Similarly, the probability that a protrusion that extended towards the - direction touches the adhesive region at the nearest neighbor has the form

$$\psi_- = g_- e^{-\lambda a_1}. \tag{4}$$

The inequality $g_+ \neq g_-$ reflects the fact that the accessible adhesive area $A_\pm$ is different for the protrusions that extended towards the + and − directions. Because of the relatively large gap between adhesive regions, the cells must exert forces that are larger than a threshold value to move from one adhesive region to another. This requires coordinated dynamics between the protrusions and retraction and therefore requires that the protrusions are stabilized. Here, we assume that this stabilization occurs with a Poisson process of rate β. Our experiments show that the stabilization time, during which a protrusion is stabilized on adhesive regions, depends on whether this protrusion is extended towards the + or - direction, most likely because of cell polarization. A protrusion that touches the (nearest) adhesive regions at the + direction is stabilized with probability

$$s_+ = 1 - e^{-\beta \tau_+}, \tag{5}$$

where τ_+ is the stabilization time for protrusions extended towards the + direction. On the - direction, the probability s_- has a stabilization time τ_-. With this model, the total number of protrusions that are extended towards the + direction is $n_+\tau_0/\tau_p$, where τ_0 is the duration that a cell stays in the same adhesive region before moving to the next region. For these protrusions, the ratio of protrusions that touch the nearest adhesive region is ψ_+, and those protrusions that touch the adhesive region are stabilized and become efficient with probability s_+. The probability that a protrusion is stabilized at the + direction rather than the - direction thus has the form

$$p_+ = C \nu_+ \tau_0 s_+, \tag{6}$$

where $\nu_+ = n_+\psi_+/\tau_p$ is the frequency of protrusions that touch the nearest adhesive region. Similarly, the probability that a protrusion is stabilized at the - direction rather than the + direction is derived in the form

$$p_- = C\nu_-\tau_0 s_-, \tag{7}$$

where the normalization constant C is deduced from

$$C^{-1} = \nu_+ s_+ \tau_0 + \nu_- s_- \tau_0, \tag{8}$$

which implies that a protrusion is stabilized either on the + or – side. One then obtains the following:

$$\begin{aligned} p_+ - p_- &= \frac{\nu_+ s_+ - \nu_- s_-}{\nu_+ s_+ + \nu_- s_-} \\ &\approx \frac{\nu_+ \tau_+ - \nu_- \tau_-}{\nu_+ \tau_+ + \nu_- \tau_-} = I_{dir} \end{aligned} \tag{9}$$

The last equation on the right hand side was derived by assuming that the rate β is much smaller than the inverse of the stabilization time (for both protrusions towards the + and - direction). This equation is indeed equal to direction index I_{dir} defined in Eq. 1 of the main text with $z_+ = \nu_+ s_+$ and $z_- = \nu_- s_-$. This provides a probabilistic interpretation of the direction index.

3.2 Persistent random walk model – long-term motion

The model aims at connecting the observed persistence and asymmetry in the +/– directions of trajectories to the fluctuation dynamics of protrusions. The persistent random walk model is defined as follows. A cell trajectory is discretized, with each elementary step defined as a transition from one adhesive motif to a neighboring motif, in either the + or – direction. We introduce the conditional transition probabilities π_{ji}, where $i,j = +,-$; these probabilities are defined as the probability that a cell performs a step in the direction j, knowing that the previous step was performed in direction i. Normalization then imposes $\pi_{+i} + \pi_{-i} = 1$; thus, only two quantities (for example, π_{++} and π_{--}) are independent. The π_{ji} *describe* the two effects responsible for the direction of migration: the asymmetry of the adhesive motifs and the direction of the previous move. The observation that $\pi_{i+} \neq \pi_{i-}$ (see Figure 5 of the main text) clearly shows that the memory of previous move, which is likely to affect the internal organization of organelles, influences the direction of the upcoming move. We now show that the main characteristics of the trajectories can be expressed in terms of the π_{ji}. The probability $\Pi_+(t)$ of observing a step in the + direction at time step t (with no knowledge of the previous step) obeys the following Markov dynamics

$$\Pi_+(t+1) = \pi_{++}\Pi_+(t) + \pi_{+-}\Pi_-(t) \tag{10}$$

The corresponding dynamics for $\Pi_{-+}(t)$ is then obtained by substituting $+ \leftrightarrow -$. The analysis of the stationary state defined by $\Pi_+(t+1) = \Pi_+(t) = \Pi_+$ yields

$$\Pi_+ = \frac{1-\pi_{--}}{2-(\pi_{++}+\pi_{--})} \tag{11}$$

The corresponding quantity Π_- is then obtained by substituting $+ \leftrightarrow -$.

4. Supplementary Movie Titles and Legends.

Movie S1 – Protrusion probing activity on an FN ratchet. Movie of an individual NIH3T3 fibroblast showing the different steps of protrusion (filopodia) activity prior to cell migration. The cell starts to fluctuate after spreading and polarizing on an adhesive fibronectin ratchet. This generates a cell front and a cell rear. The colored arrows (blue and green) highlight the probing of the protrusions on the neighboring adhesive motifs. The yellow arrows indicate the start of the cell spreading and migration and the retraction at the back of the cell. Acquisition time: 1 image/30 seconds. Time in hh:mm:ss. (Scale bar: 50 μm).

Movie S2 – Protrusion probing activity on a triangle with 2 symmetric rectangles. Protrusion (filopodia) activity of an NIH3T3 cell spread on an FN triangle with rectangle-shaped neighboring motifs on both sides. The colored arrows (blue and green) highlight the probing of the protrusions on the neighboring adhesive motifs. The yellow arrows indicate the start of cell spreading and migration. Acquisition time: 1 image/30 seconds. Time in hh:mm:ss. (Scale bar: 50 μm).

Movie S3 – Protrusion probing activity on a spot with 2 symmetric neighboring rectangles. Protrusion (filopodia) activity of an NIH3T3 cell spread on an FN spot with rectangle-shaped neighboring motifs on both sides. The colored arrows (blue and green) highlight the probing of the protrusions on the neighboring adhesive motifs. The yellow arrows indicate the start of cell spreading and migration. Acquisition time: 1 image/30 seconds. Time in hh:mm:ss. (Scale bar: 50 μm).

Movie S4 – Fluctuating NIH3T3 cell on a fibronectin spot pattern. Movie of an individual NIH3T3 fibroblast fluctuating for 48 hours from one fibronectin spot (in red) to the neighboring ones, crossing the PLL-g-PEG blocked regions, and changing its direction of migration. Acquisition time: 1 image/5 minutes. Time in hh:mm. (Scale bar: 100 μm).

Movie S5 – NIH3T3 cell motion on a sequence of triangular fibronectin patches. Movie of an individual NIH3T3 fibroblast for 30 hours plated on a sequence of micropatterned fibronectin triangular patches (in red). The NIH3T3 cell fluctuates + and - at the beginning of the movie from one fibronectin triangle to the neighboring ones, crossing the PLL-g-PEG blocked regions. Then, the cell migrates directionally in the + direction. Acquisition time: 1 image/5 minutes. Time in hh:mm. (Scale bar: 100 μm).